

Supporting Information

Suppressed energy transfer between different rare earth ions to obtain enhanced and tuned fluorescence by using Janus nanofibers

Ping Wu, Qianli Ma,* Wensheng Yu, Jinxian Wang, Guixia Liu and Xiangting Dong*

School of Chemistry and Environmental Engineering, Changchun University of Science and Technology, Changchun 130022, China.

1. XRD analyses.

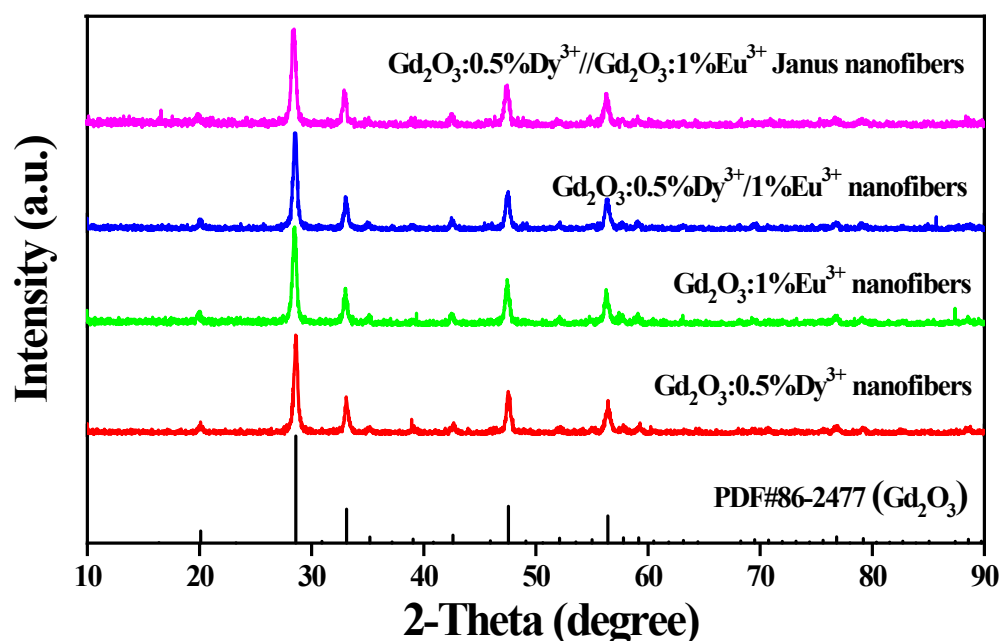


Fig. S1 XRD patterns of the samples.

Figure S1 shows the XRD patterns of $\text{Gd}_2\text{O}_3:\text{Dy}^{3+}$ nanofibers, $\text{Gd}_2\text{O}_3:\text{Eu}^{3+}$ nanofibers, $\text{Gd}_2\text{O}_3:\text{Dy}^{3+}/\text{Eu}^{3+}$ nanofibers and $\text{Gd}_2\text{O}_3:\text{Dy}^{3+}/\text{Gd}_2\text{O}_3:\text{Eu}^{3+}$ Janus nanofibers. The positions and strength ratio of the XRD diffraction peaks of the prepared samples are highly consistent with those of standard card (PDF#86-2477) of cubic phase Gd_2O_3 . It can be seen that the doping of Dy^{3+} or Eu^{3+} does not visibly change the crystal structure of Gd_2O_3 .

2. Fluorescence analyses.

Figure S2a and S2b shows the excitation and emission spectra of $\text{Gd}_2\text{O}_3:\text{Dy}^{3+}$ nanofibers doped with different amounts of Dy^{3+} . When 486 nm is chosen as the monitoring wavelength, a wide excitation band assigned to $\text{O}^{2-} - \text{Dy}^{3+}$ charge transfer band, with the maximum at *ca.* 210 nm, can be observed in the excitation spectra, as revealed in Fig. S2a. Besides, some relatively weak and

sharp excitation peaks also can be seen, which can be ascribed to the transitions of $^8S_{7/2} \rightarrow ^6D_{9/2}$ (255 nm), $^8S_{7/2} \rightarrow ^6I_{9/2}$ (272 nm), $^8S_{7/2} \rightarrow ^6P_{5/2}$ (300 nm) of Gd^{3+} and $^6H_{15/2} \rightarrow ^6P_{7/2}$ (350 nm), $^6H_{15/2} \rightarrow ^6P_{5/2}$ (364 nm), $^6H_{15/2} \rightarrow ^4I_{13/2}$ (386 nm) of Dy^{3+} . The above results verify the energy transfer from matrix and Gd^{3+} to Dy^{3+} . The transitions of $^4F_{9/2} \rightarrow ^6H_{15/2}$ (486 nm) and $^4F_{9/2} \rightarrow ^6H_{13/2}$ (578 nm) of Dy^{3+} are observed in the emission spectra shown in Fig. S2b when the samples are excited by 210 nm ultraviolet light. Furthermore, it can be seen that the fluorescence intensity of $Gd_2O_3:Dy^{3+}$ nanofibers is increased first and then decreased with doping more Dy^{3+} . The decreased fluorescence intensity is due to fluorescence quenching. As the doping concentration of Dy^{3+} is 0.5%, the $Gd_2O_3:Dy^{3+}$ nanofibers display the highest fluorescence intensity.

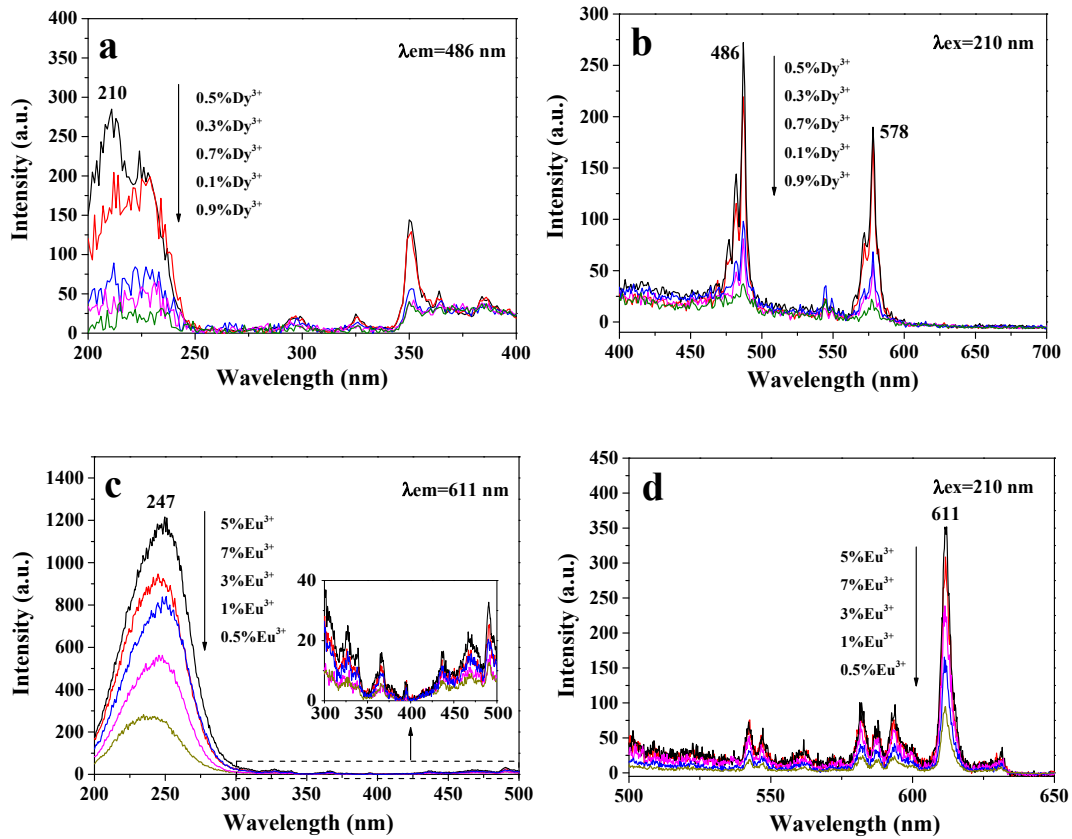


Fig. S2 (a, c) Excitation and (b, d) emission spectra of (a, b) $Gd_2O_3:Dy^{3+}$ nanofibers and (c, d) $Gd_2O_3:Eu^{3+}$ nanofibers.

Figure S2c and S2d reveal the excitation and emission spectra of $Gd_2O_3:Eu^{3+}$ nanofibers. As shown in Fig. S2c, the excitation spectra of $Gd_2O_3:Eu^{3+}$ nanofibers monitored at 611 nm also display a wide and strong excitation band with the center at 247 nm, which is attributed to $O^{2-} - Eu^{3+}$ charge transfer band. In addition, the transitions of $^7F_0 \rightarrow ^5H_3$ (322 nm), $^7F_0 \rightarrow ^5D_4$ (365 nm), $^7F_0 \rightarrow ^5L_6$ (395 nm), $^7F_0 \rightarrow ^5D_3$ (437 nm), $^7F_0 \rightarrow ^5D_2$ (465 nm) and $^7F_0 \rightarrow ^5D_1$ (490 nm) of Eu^{3+} are also observed. As for the emission spectra of $Gd_2O_3:Eu^{3+}$ nanofibers shown in Fig. S2d, 210 nm is selected as the excitation wavelength rather than 247 nm because even though the Eu^{3+} is not excited in the most effective circumstance, the emission intensity of $Gd_2O_3:Eu^{3+}$ nanofibers excited by 210

nm ultraviolet light is still much higher than that of $\text{Gd}_2\text{O}_3:\text{Dy}^{3+}$ nanofibers, and in order to acquire optimized white fluorescence from $\text{Gd}_2\text{O}_3:\text{Dy}^{3+}/\text{Eu}^{3+}$ nanofibers and $\text{Gd}_2\text{O}_3:\text{Dy}^{3+}/\text{Gd}_2\text{O}_3:\text{Eu}^{3+}$ Janus nanofibers, the excitation wavelength should be most effective for Dy^{3+} . Under these premises, the investigation on using 210 nm ultraviolet light to excite $\text{Gd}_2\text{O}_3:\text{Eu}^{3+}$ nanofibers is more meaningful. As seen from Fig. S2d, the transitions of $^5\text{D}_1 \rightarrow ^7\text{F}_1$ (538 nm), $^5\text{D}_1 \rightarrow ^7\text{F}_3$ (582 nm), $^5\text{D}_0 \rightarrow ^7\text{F}_1$ (594 nm), $^5\text{D}_0 \rightarrow ^7\text{F}_2$ (611 nm) of Eu^{3+} are identified in the emission spectra under 210 nm excitation, and the quenching concentration of Eu^{3+} is 5%.

The normalized time-resolved fluorescence spectra of $\text{Gd}_2\text{O}_3:\text{Dy}^{3+}/\text{Gd}_2\text{O}_3:\text{Eu}^{3+}$ Janus nanofibers and $\text{Gd}_2\text{O}_3:\text{Dy}^{3+}/\text{Eu}^{3+}$ nanofibers with different concentration of Eu^{3+} are presented in Fig. S3 and used to calculate the lifetime. The calculated decay lifetimes are listed in Table 1 of the main text. The curves are also plotted in semi-Log form to more intuitively show the decay rates of lifetimes, as seen in Fig. S4.

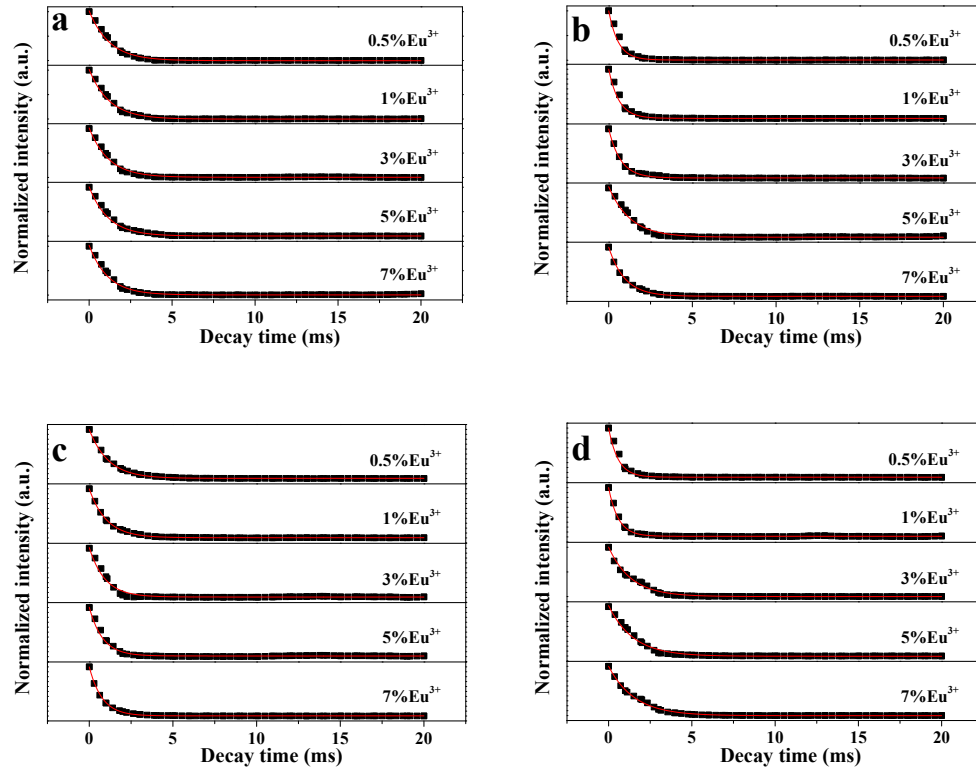


Fig. S3 Time-resolved curves (black dots) and fitting curves (red curves) of (a, c) Dy^{3+} (486 nm) and (b, d) Eu^{3+} (611 nm) in (a, b) $\text{Gd}_2\text{O}_3:\text{Dy}^{3+}/\text{Gd}_2\text{O}_3:\text{Eu}^{3+}$ Janus nanofibers and (c, d) $\text{Gd}_2\text{O}_3:\text{Dy}^{3+}/\text{Eu}^{3+}$ nanofibers.

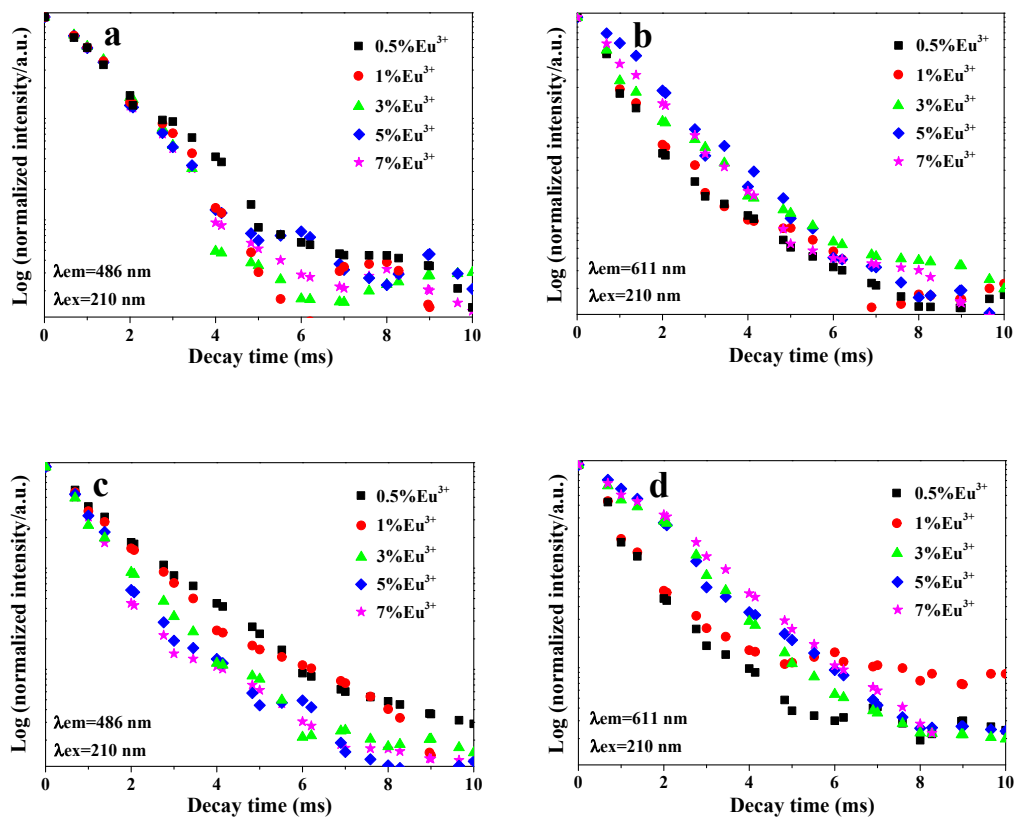


Fig. S4 Natural logarithmic scale on the Y-axis plots of (a, c) Dy^{3+} (486 nm) and (b, d) Eu^{3+} (611 nm) in (a, b) $\text{Gd}_2\text{O}_3:\text{Dy}^{3+}/\text{Gd}_2\text{O}_3:\text{Eu}^{3+}$ Janus nanofibers and (c, d) $\text{Gd}_2\text{O}_3:\text{Dy}^{3+}/\text{Eu}^{3+}$ nanofibers.